2023

Tensiography and Liquid Drop Metrology

David Kennedy
Technological University Dublin, david.kennedy@tudublin.ie

Des Carbery
SETU

Norman McMillan
SETU

Recommended Citation

Kennedy, D., Carbery, D., & McMillan, N. (2023). Tensiography and Liquid Drop Metrology. HDMT. DOI: 10.21427/GDPK-8S40

TENSIOGRAPHY AND LIQUID DROP METROLOGY

David M. Kennedy[1], Des Carbery and Norman McMillan

[1] Technological University Dublin, Ireland

Professional paper / Stručni rad

Abstract

This research focused on drop metrology and the use of camera technology and vibration analysis influence on theoretical and practical tensiography. Drop shape and Tensiography are explained and how they relate to each other. Studies shows a relationship between vibration frequency and surface tension of liquids. However they also reveal the need for a theoretical understanding of the vibration tensiotrace of drops. Camera studies on large diameter dropheads used in tensiography are explored. Various image analysis methods were investigated for determining drop shape from camera images. Examination of the digital image reveals measurement issues. High speed camera images reveal new details of the drop separation process. An examination of drop modelling methods from camera images and the principles of such modelling were undertaken. Camera studies were developed which enabled the practical investigation of edge-detection. The theory developed links the drop shape with the tensiotrace of drops examined.
The ray tracing method of the modelling of drop shape would have to be consolidated by establishing a definitive relationship between drop shape and the tensiotrace. This lead to acquiring photo images of real drops to get the profile of its edge or the drop shape.
Various methods are used and assumptions are made in finding the edge of a drop from a photo image, in particular to the measurement of length, radii and angles.

***Keywords**: Tensiography, Liquid Drop analysis, Ray tracing.*

Corresponding author: David Kennedy, david.kennedy@tudublin.ie

1. INTRODUCTION

A drop rheometer is an instrument to measure the surface properties of liquids. The scientific study of liquid surfaces dates from Leonardo da Vinci [1] who studied the rise of a liquid up a capillary tube. Eggers [2] presented a history of the study of drop formation, observing the static and dynamic state of a drop.

The objectives of the work were as follows:

i. to investigate the process of a separating drop,
ii. to link the theoretical and experimental observations of vibrating drops.
iii. to investigate the dimensional invariance of tensiography in surface science,
iv. to examine the modelling of large drops,

The authors worked on the design of a rheometer based on McMillan's tensiography [3] studies. Vibration tensiotraces (the signal output of light reflected around the inside of a vibrating drop) were also examined. Using a liquid drop for measurement originates from 1864 with the work of Tate [4] who experimentally demonstrated a drop as a reproducible measure of weight. Work by Rayleigh [5] on "the size of drops" advanced these studies further. In 1854 Tyndall [6] first presented his demonstrations of the reflection of light inside a jet of water (Fig. 1). "Light on reaching the limiting surface of air and water was totally reflected." This is shown later, to be related to tensiography.

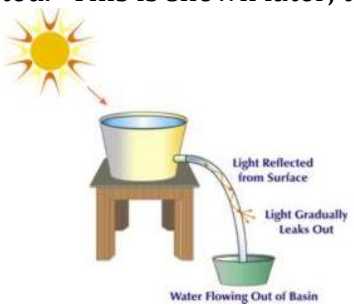

Fig. 1: Depiction of Tyndall's experiment of light reflection in a jet of water.

2. Tensiography Equipment Developed and mode of operation

Tensiography is a relatively new science and the first aspects of this was developed in the optical domain. It is based on graphical methods of signal analysis. The optical temporal signal is derived from light coupled around the inside of a growing pendant drop. The drophead (see Fig. 5) contains two optical fibres within the growing drop. The light is injected into the drop by the source fibre in the drophead and a detector at the end of the collector fibre records the entire drop characteristics from remnant drop initiations until the mature drop separates.

The first multispectral tensiograph recordings with CCD detectors were made in 1992 by McMillan et al [3]. In recent times, a tensiograph instrument has been used in many areas such as characterization of all types of liquids and water quality analysis.
The instrument arrangement is shown in Fig. 2. The liquid to be analysed is pumped via the liquid delivery tube **c** to the drophead **d** using a motor stepper pump **b** and a pendant drop grows at a uniform volume rate (isochoric) in size until it separates from the drophead. Throughout this process, light from an LED, **f** is injected into the drop through the source-fibre and the reflected signal, picked up by the collector-fibre is transmitted to a photodiode **h**. The amplification of the low photocurrent into an adequate voltage signal is necessary before the signal is passed to an acquisition board [an electronic system

based on a programmable interface controller (PIC) and other suitable electronics hardware] incorporated in a personal computer (PC) **i**. The optical eyes **g** enable the signal to be scissored – the initial trigger occurs when the initiation drop falls through the optical eye and triggers the start of the data acquisition. This indicates when the measurement drop has arrived on the drophead and then the data acquisition continues until this drop falls off the drophead and the second trigger locates precisely the ending of recording of the tensiotrace (a data set recorded over the life cycle of the drop). Two-stage anti-vibration mounts **l** and **m** protect the drop from vibrations. The analogue to digital converter (ADC) of the acquisition board converts the analogue voltage (amplified optoelectronic signal from the detector) into a digital signal, which is then stored for later analysis.

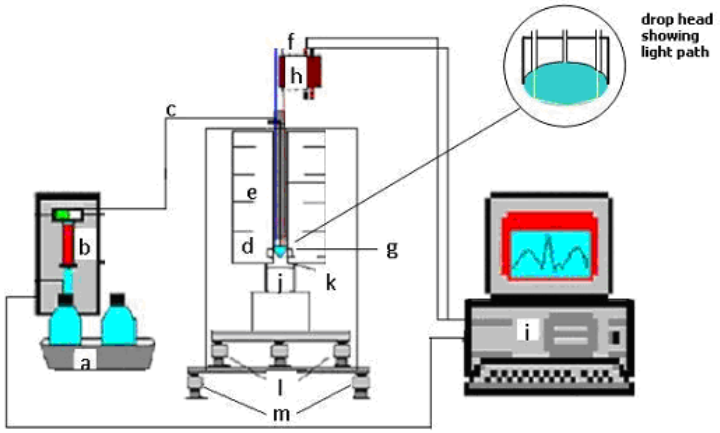

	Description		Description
a	Samples for analysis	**h**	Detector
b	Stepper-motor-pump	**i**	Computer
c	Delivery tube	**j**	Chamber to ensure saturation of atmosphere
d	Drophead	**k**	Temperature sensors
e	Temperature control	**l**	Auto-levelling drives
f	Light source	**m**	Anti-vibration balancing feet
g	Optical eyes		

Fig. 2: Schematic diagram of the tensiograph instrument.

The source-detector employs a CCD (charged couple device) or CMOS (complementary metal oxide semi-conductor) detector in conjunction with a spectral source such as fibre deuterium, xenon, halogen or tungsten sources. Such a system provides a spectral array of tensiotraces, one for every measurement wavelength. The temperature sensor must stabilise. Once the set value is reached measurements can commence. The sensor performance repeatability is checked to see if it is within the allocated tolerance. The drop head must be wetting i.e. the drop is forming over the entire drop head surface. Every sample is degassed before being analysed with the instrument. This is done to remove any bubbles within the sample.

The key concept of the tensiograph is that all the various physical and chemical processes that modulate the coupled light in the drop produce a signal, which is unique in a theoretical sense for every specific combination of properties of the liquid under test (LUT). These processes include partial reflection of the light beam inside the pendant drop, absorption of the light from chromophores in the liquid, scattering of the light from turbid particulate matter and changes in the emission angle from the source fibre. The detected light intensity is amplitude modulated during the life cycle of a drop i.e. the

reflecting surface of the inner drop changes continuously. Fig. 3 shows the characteristic features of the tensiotrace of a liquid.

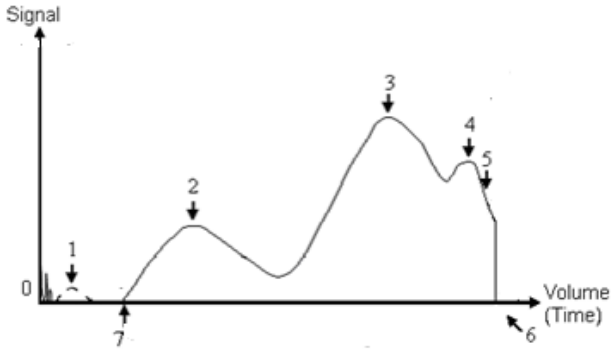

Label	Description
0	Separation vibration
1	First-order peak
2	Rainbow peak
3	Tensiopeak
4	Shoulder peak
5	Separation peak
6	Drop period
7	Rainbow peak commencement

Fig. 3: Tensiotrace showing the trace features associated with drop.

The x-axis can be either volume or time as both are equivalent for constant volume delivery from stepper pumps. Two measurands are noted: tensiopeak period or time to tensiopeak (t_3) and time of drop period (T_1). The rainbow peak height and position in the tensiotrace is a good measure of refractive index. The height of the tensiopeak provides a good measurand for determining the colour and/or turbidity of the solution in that the peak decreases respectively with the increasing absorptive or scattering power of the liquids. The drop period can be used to give a good measure of the surface tension/density ratio. The principal use of the tensiograph is as a fingerprinting technique. It has been demonstrated, over a considerable period of time that the combination of the complex of physical and chemical properties of the drop ultimately defines the form of the tensiotrace and thus the tensiotrace provides a very sensitive fingerprint technique for liquids.

3. Drop shape

Fig. 4 shows two full size 9mm drops of water and ethanol.

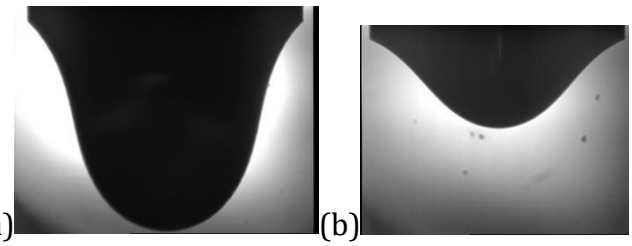

Fig. 4: Drops of (a) water and (b) ethanol on a 9mm drophead

The water shape is often described as “thimble shape” and the alcohol one as “bell shape”. The shape is governed by many factors including the liquid properties, such as density and surface tension. One affects the downward force and the other the upward force on the drop. The ratio of these two liquid properties affects the drop shape. Surface tension (γ) is defined [1] as “the force acting in the surface of a liquid, tending to minimize the area of the surface. Surface forces, or more generally, interfacial forces, govern such phenomena as the wetting or non wetting of solids by liquids, the capillary rise of liquids in fine tubes and wicks, and the ***curvature*** of free-liquid surfaces”. The relationship between interfacial pressure ΔP across an interface and its interfacial tension (γ) is fundamental to this curvature or drop shape. This relationship was initially presented by Laplace:

$$\Delta P = \gamma\left[\frac{1}{R_1}+\frac{1}{R_2}\right] \quad (1)$$

where R_1 and R_2 are the principal radii of curvature at the drop surface edge. These radii are shown in Fig.5. R_1 and R_2 are orthogonal.

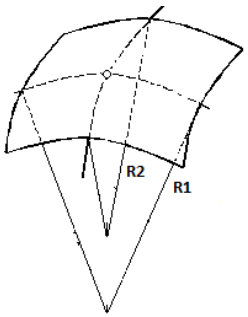

FigError! No text of specified style in document.**. 5: Principal radii of curvature of a drop surface**

Rays are traced around the inside of the drop (Fig. 6) and obey the law of reflection given the Fresnel reflection coefficient (which depends on the refractive index) for the angle of incidence of the ray and the drop surface. Colour (measured in a liquid by either absorbance or transmission) and turbidity are both dimensionless quantities. The model also includes attenuation from absorption based on the length of the ray that couples between source and collector fibre. If the ray eventually strikes the detector fibre within the acceptance angle of the fibre, its intensity is added to the total.

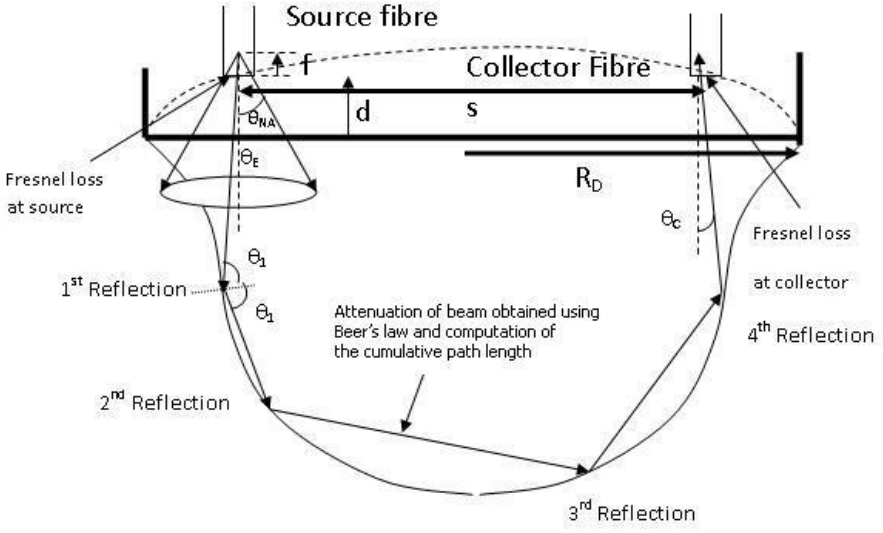

Fig. 6: Simple illustration of the physics of the ray tracing model.

If the ray can propagate up the fibre then the percentage of photons that have been coupled is calculated from all the reflection coefficients. The signal is then computed from the sum of all the rays that make up the spiral. The drop-volume is then increased incrementally, a new shape computed and another ray tracing procedure executed. The signal then at this drop-volume is obtained and the whole procedure is stepped until the drop falls off. The position at which the drop falls is taken to be the maximum volume possible for a drop.

4. Vibration of pendant drops

Spherical drops vibrate in a simple way and the problem of these drop vibrations was analytically solved by Rayleigh [5] who showed that the drop vibrated with a single mode of period (T_V) given by:

$$T_V = (3\pi\rho V / 8\gamma)^{1/2} = 2\pi (\rho r^3 / 8\gamma)^{1/2} \quad (2)$$

where;
V is the volume of the drop
γ is the surface tension of the drop
ρ is the density of the drop
r is the drop radius

This result shows that the drop vibration period decreases with the volume and density of the liquid and increases with surface tension. Vibrations on the surface of the drop modulate light injected inside the drop. Light will be injected into the drop as a cone of light from the source fibre and will reflect from a range of positions on the drop base. Ambient conditions are important to drop shape. The physical properties of the liquid under test (LUT) vary with temperature. In this regard the ratio of surface tension(γ)/density(ρ) is the factor that determines the drop shape variation.

5. Photographic methods for surface tension.

Ferguson [7] in 1911 used photographic methods of analysing pendant drops concentrating on the apex of the drop. His main concern was to test the equations that fit the drop rather than produce a practical tool for surface tension measurements. The experimental basis for the pendant drop measurement in 1979 was still very traditional as can be gauged by the review chapter of Ambwani and Fort [8]. A modern generation of drop imaging techniques began with standard TV cameras in the 1980s and amongst the first was Girault et al [9] who reported measurement accuracies of better than 1% based on measuring at the point of inflexion at which there is only one principal radius. Hauser [10] first dealt with the issues of measuring drops with cameras in 1936, and a most recent review of camera measurements on drops was done by Neumann [11].

6. Experimental Studies in Drop Metrology

Drop images were obtained from camera systems. Fig. 7 is a schematic of the pendant, satellite and primary drops.

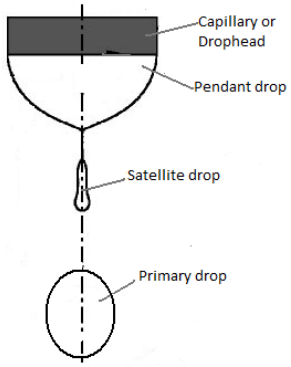

Fig. 7: Pendant, satellite and primary drops

The events leading to these separate drops can be termed a drop separation process. The physics of an equilibrium process would force the drop to form into a spherical shape, but is of course acted on by many forces including force of gravity, surface tension, surface waves, fields of flow within the drop and external friction. The quartz drophead used is shown in Fig. 8. It consists of a capillary, through which the liquid is delivered to the quartz drophead. It also includes an optic fibre for the light source when required and a receiving optic fibre.

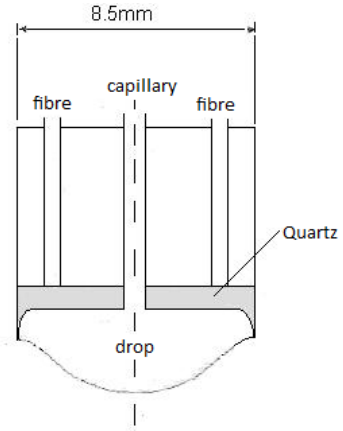

Fig. 8: Quartz drophead

The pump speed was set at 200 which gave a flow rate of 1.25µl/s. A drop was formed on the drophead and images of the drop were captured just before the time that the drop became unstable and continued to be taken through the drop separation process. A Photron camera (Fastcam SA1.1 model) was used for capturing the images. The maximum resolution of the camera was 1000*1000 pixels and the images were taken at 5000 fps and 5400 fps (frames per second). Table 1.1 shows the liquid properties[i] of the methanol and water drops.

Table 1.1 Liquid properties of the drops under test

Properties	Water	Methanol
Density (kgm^{-3})	998.6	791.1
Surface tension (mNm^{-1})	73.05	24.05
Viscosity (cP)	1.002	0.6

The following camera images were taken:

i. Individual camera images of two separating water drops
ii. Individual camera images of two separating methanol drops
iii. Synchronised images of the separating water drops
iv. Synchronised images of the separating methanol drops
v. Camera images of the contact edge of the methanol drop at the drophead

The camera speeds for the drop images are shown in Table 1.2.

Table 1.2 Camera speeds for drop images

Drop identity	Camera speed (fps)
Water 1 (C001H001S0002)	5,400
Water 2 (C001H001S0003)	5,000
Methanol 1	5,000
Methanol 2	5,000

6.1 Camera images

Figs. 9 i 10 show images of the typical drop separation process in the case of water and methanol. The frame numbers are given so that the time between images can be calculated on the basis of the camera speed.

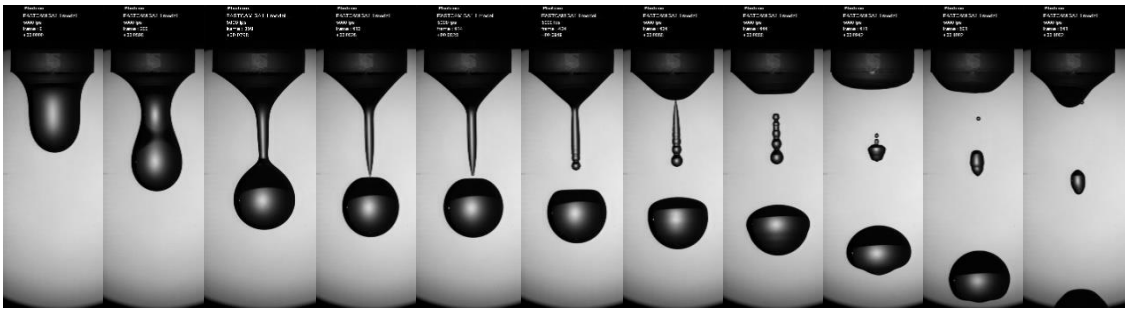

Fig. 9: Images captured during the separating process of water drop. Frames 0, 299, 399, 413, 414, 424, 434, 444, 471, 501, 541.

At first the full drop is shown, then necking showing positive and negative radii of curvature of the drop edge. Next, the almost cylindrical midsection reduces to a pinhead before the primary drop separates. At this stage the pendant drop is fully extended before pulling back upwards when the satellite drop separates. As the satellite falls, a daughter satellite separates upwards and continues until it contacts the pendant drop when it rebounds off the pendant drop. A similar observation to the latter was made in 1936 by Hauser et al [10] used a high-speed motion picture camera (1200 f.p.s) to observe the drop separations from a 4.58mm capillary. Fig. 10 shows images captured during the separating process of a methanol drop. The process is generally similar to the water set but the proportions of size are very different.

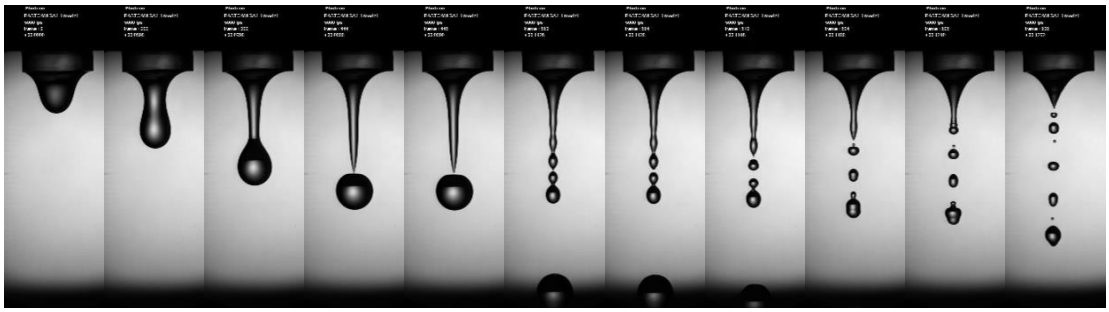

Fig. 10: Images captured during the separating process of a methanol drop. Frames 0, 299, 399, 444, 445, 563, 564, 573, 594, 605, 636.

Fig. 11 shows another water drop for comparison with Fig. 9. The separating process is similar to that shown previously in Fig. 9, and includes a daughter satellite also.

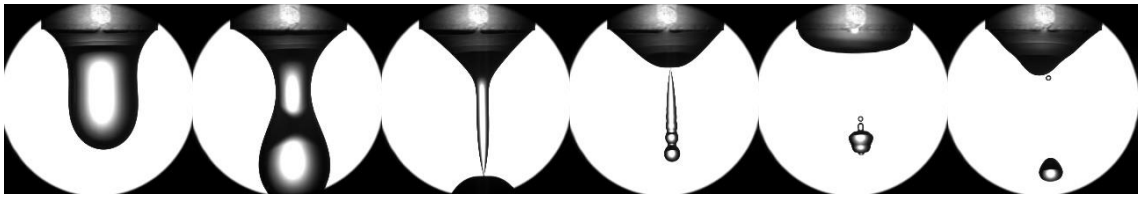

Fig. 11: Water drop 1. Frames 1, 251, 350, 374, 413, 472
(a) (b)

The profile of the pendant drop at this stage is varying between hemispherical and conical. The profile of the pendant water drop could be described as being between hemispherical and conical but not the methanol drop. However, this is not the case at any stage with the pendant methanol drop. For the methanol drop separation images, they have a greater number of separated drops. Fig. 12 shows this application.

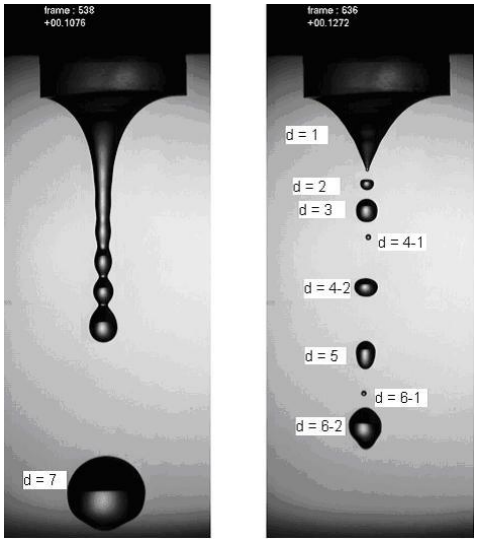

Fig. 12: Methanol drops identified

The first frame shows the separated primary drop and the initial formation of the satellite drop. The second frame shows the further separation of the satellite drop. Both frames are required because the primary drop has disappeared from the camera view in the second frame.

6.2 Drop volumes

Drop volumes can be calculated from the images and the results for one water and one methanol drop are shown in Table 1.3.

Table 1.3 Drop volumes for water and methanol

Water drop 2		Methanol drop 1	
Drop	**Volume (µl)**	**Drop**	**Volume (µl)**
d1	70	d-1	60
d 2-1	0.02	d 2	0.19
d 2-2	2.07	d-3	1.23
d 3	114.7	d 4-1	0.01
		d 4-2	1.01.0
		d 5	1.23
		d 6-1	0.01
		d 6-2	3.87
		d 7	46.7

6.3 Detail of water drop images.

Fig. 13 shows a detailed selection at an early stage prior to separation.

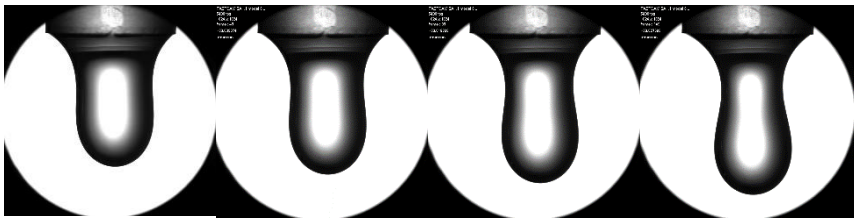

Fig. 13: Water drop 1 Frames 1, 50, 100, 150, 200.

In the first image, the whole drop is in equilibrium under the action of the force of gravity and surface tension. As liquid is added, the drop changes shape to accommodate the balancing surface tension force and the drop separation process commences before the final image in this selection. The shape of the first image in this selection could be closely described as having a lower cylindrical shape with a hemispherical end. It gradually changes shape converging towards an obvious weaker section ("necking"). Fig. 14 shows the water drop images at a further stage.

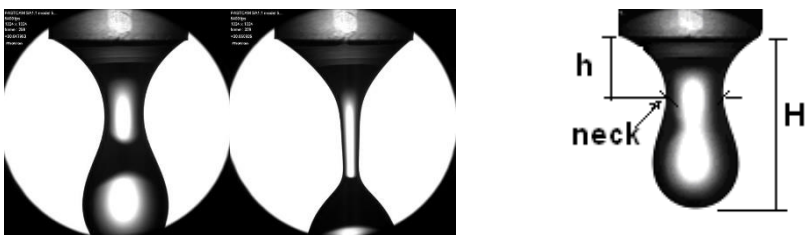

Fig. 14: Water drop "necking" frames 260, 330.

Necking has continued here and the second image shows almost cylindrical necking.

The height (H) for water drop1 as the primary drop separates was measured at 16.68mm. The unbalanced upward surface tension force causes this 'pull back'. Simultaneously, the top of the primary drop 'flattens' for the same reason. Then the top of the satellite drop reduces to a needlepoint, due to the force of gravity before separating. Also at this stage the 'pull back' effect can be seen on the pendant drop, changing its fully extended cone shape.

The images in Fig. 15 show the continued path of the second satellite drop. This satellite continues upward until it meets the surface of the pendant drop, a vertical distance of 4.8mm.

Fig. 15: Rebound of the satellite drop.

At this contact the surface attraction is not strong enough to cause them to coalesce together and the second satellite rebounds away from the pendant drop. The speed of the satellite before contact is calculated as 275 mm/s and after contact 367 mm/s.

7. Oscillation of the water satellite drop

The water satellite drop moves downwards due to gravity. The calculated volume of this drop was 2µl. The images shown in Fig. 16 clearly show its changing shape, oscillating about its equilibrium spherical shape as it falls. These events are reproducible. Satellite drops have similar necking effects and the satellite drop shapes are similar. The satellite drops are projected upwards.

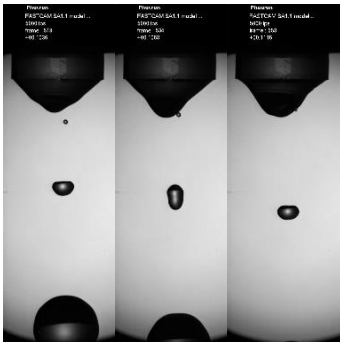

Fig. 16: Water satellite drop changing shape.

7.1 Detail of methanol drop images.

The methanol drop images are presented from the beginning of the separation process and are shown in Fig. 17.

Fig. 17: Methanol drop. Frames 0, 171, 269, 329, 395.

The process is similar to that of the water drop, however ratios of neck diameter to height are different because of the liquid properties. The height (H) of the drop as the primary drop separates was measured at 16.4mm, compared with the same water drop measurement of 16.68mm. The weight of the primary drop combined with the liquid properties is a contributing factor to this height (H). The weights of the primary drop for methanol and water drops are calculated at 36.96μN and 114.53μN respectively.

7.2 Methanol satellite drops.

Fig. 18 shows some of the images from the separation of the primary drop to the separation of the first satellite drop. The comments about the forces involved at this stage in the water drop separation process, are again relevant here.

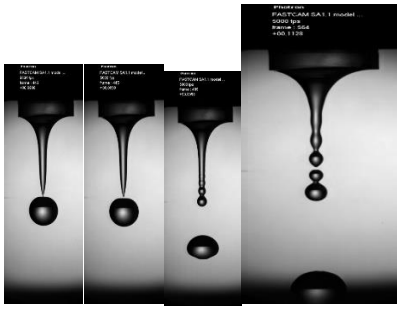

Fig. 18: Formation of the methanol satellite drop. Frames 443, 445, 499, 564.

The needlepoint end of the satellite drop changes to a rounded end as the unbalanced surface tension force 'pulls' the end upwards. The downward force of gravity retards the upward motion of this end. The resulting compression and oscillation of the satellite sections eventually cause the separation shown in frame 564. Further separations of the methanol satellite drop are shown in Fig. 19.

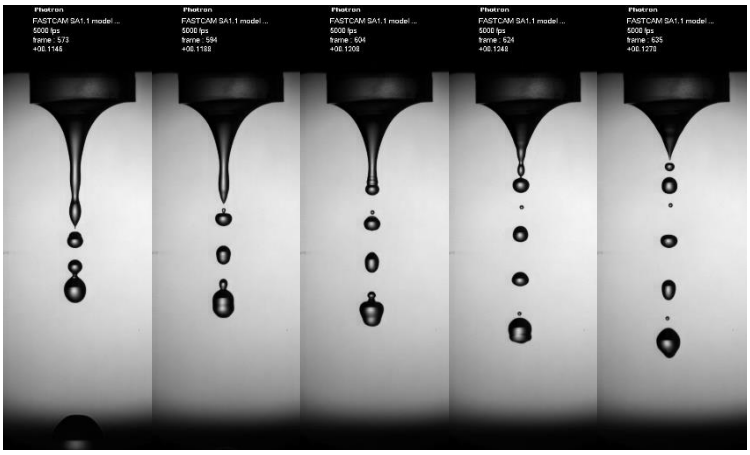

Fig. 19: Separations of the methanol satellite drop. Frames 573, 594, 604, 624, 635.

Four further satellite drops separate and from two of these, drops are ejected upwards. Frame 635 shows these satellite drops in descending order d2, d3, d4-1. d4-2, d5, d6-1 and d6-2.

8. Oscillation of methanol satellite drop (d5).

The methanol satellite drop (d5) moves downwards due to gravity. The calculated volume of this drop was 1.2µl. The images shown in Fig. 20 clearly show its changing shape, oscillating about its equilibrium spherical shape. The methanol primary drop (d7) is the first drop to separate in the drop separation process. The calculated volume of this drop was 46.7µl.

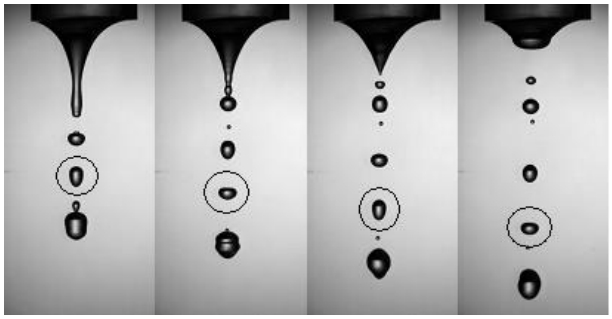

Fig. 20: Satellite drop d 5 changing shape Plates 597, 618, 636, 655.

Fig. 21 shows a series of images of this drop from the beginning of its separation.

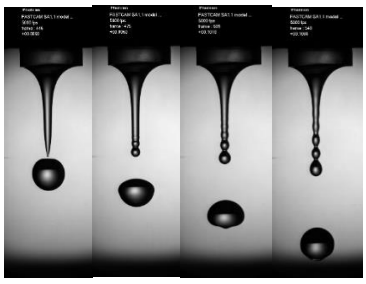

Fig. 21: Methanol primary drop. Frames 446, 476, 506, 541.+

9. Drop vibration rheometry

A pendant drop was vibrated resulting in the recording of a vibration tensiotrace as shown in Fig. 22.

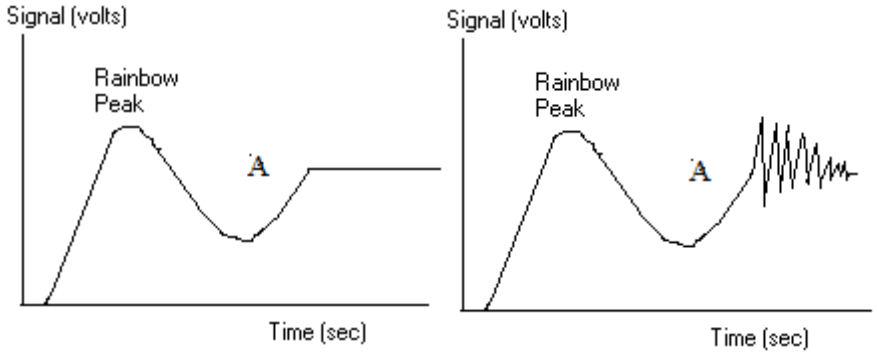

Fig. 22: Vvibration tensiotrace

The left figure shows the tensiotrace that results when the pump is stopped at point A. From this point, the tensiotrace is a horizontal line as the light reaching the receiver is constant. When the drop is vibrated at this stage the right diagram shows the resulting trace (commencing at A) now termed a vibration tensiotrace.

9.1 Excitation of the drop

A shock was applied to the drop by placing a brass cap on top of the drop head and dropping a steel ball onto it. It was established that a 10mm steel ball from a height of 135mm resulted in a vibration of suitable scale size. A second method consisted of an electronic hammer which applied a mechanical shock to the side wall of the drophead holder. The vibration tensiotrace appears to give a fingerprint of the surface properties of the liquid under test. It was found experimentally that the form of the trace varies with the drop volume. Fig. 23 shows a series of vibration tensiotraces for ethanol recorded at different drop volumes but with the head levelled and with the same mechanical excitation. All traces were recorded at 20^0 C.

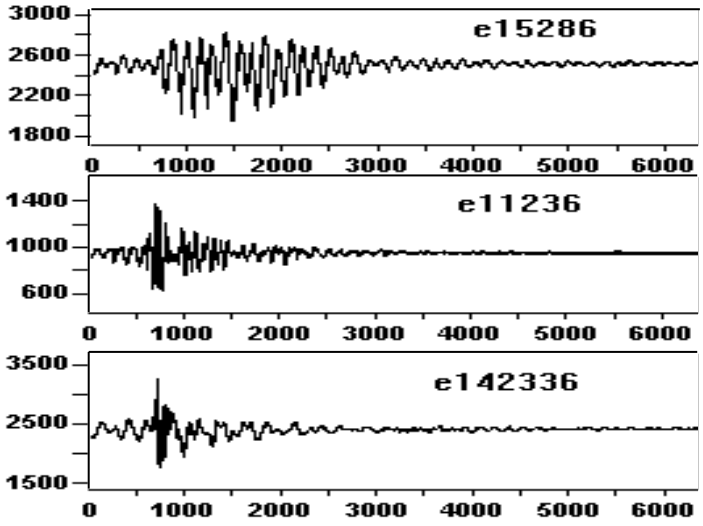

Fig. 23: Vibration tensiotraces of ethanol solutions

For **e15286: e** indicates that it is **e**thanol liquid, the **1**st drop, vibrated the **5**th time, drop volume **28**secs (pump stopped after this time), and the vibration is shown over a **6** sec range. When related to pump speed, the pump delivers 35µl in 28s. Fig. 24 shows vibration tensiotraces for 3 repeated excitations of the same water drop. There is a high degree of visual similarity of the vibration tensiotraces.

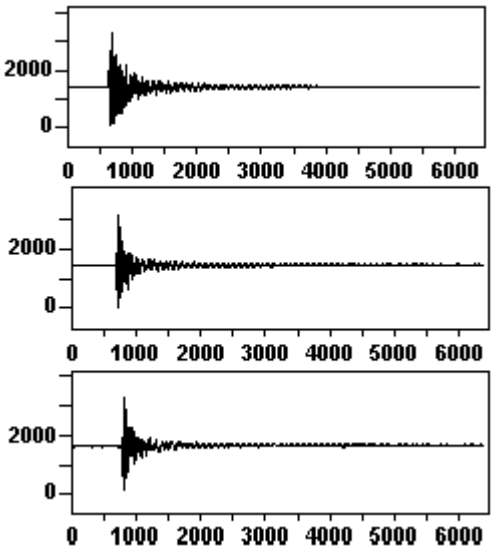

Fig. 24: Vibration tensiotraces of a water drop

Fig. 25 shows vibration tensiotraces of a drop of 80% ethanol solution. These are the result of 3 different excitations of the same drop. They show variations in experimental amplitude but similarity in general shape. The first halves of the traces are similar but show a reducing number of peaks. The amplitudes in the second halves are different.

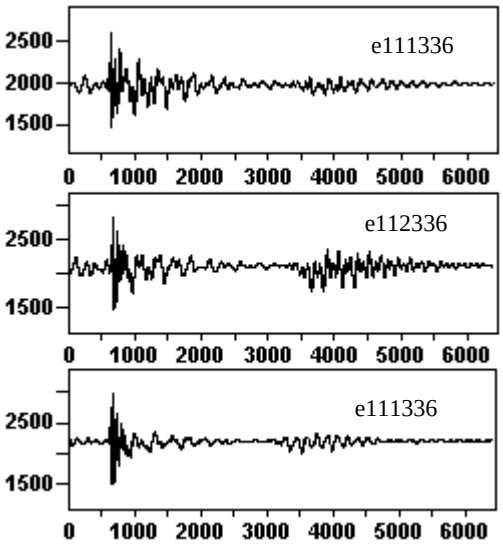

Fig. 25: Vibration tensiotraces of the same ethanol drop.

Any differences may be the result of the difficulty of reproducing a similar excitation of the drop.

Discussion and Conclusions

The analysis of the ethanol vibration tensiotraces showed reproducibility in results. This analysis could be extended further to consider frequency peaks and amplitudes and also to other liquids. However, the analysis is complex. An improved laboratory instrument would yield a more exact definition of this convergence. Vibration tensiotraces of liquids are unique to the liquids under test and produce a fingerprint. Mechanical vibrations produce the vibration traces with a drop of a constant size and these are reproduced.
A surface drop rheometer based on these experiments and results could be designed and developed. The instrument design would include the following:
(a) A method of forming the drop
(b) A means of excitation of the drop
(c) An ability to vary the drop tilt angle
(d) Instrumentation for analysing the vibration.

References

[1] Maxwell, J. (1878). "Capillary action. Encyclopedia Britannica, 9th edn, vol. V, 67. Charles Scribner."
[2] Eggers, J. (2006). "A brief history of drop formation." Advances in Mechanics and Mathematics **12**: 163.
[3] McMillan, N., F. Fortune, et al. (1992). "A fiber drop analyzer: A new analytical instrument for the individual, sequential, or collective measurement of the physical and chemical properties of liquids." Review of Scientific Instruments **63**: 3431.
[4] Tate, T. (1864). "On the magnitude of a drop of liquid formed under different circumstances." Phil. Mag **27**: 176–180.
[5] Rayleigh, L. (1899). "Investigations in capillarity." Phil. Mag **48**(321-330): 222.
[6] Tyndall, J. (1854). On some phenomena connected with the motion of liquids. Proc R Inst Great Britain.
[7] Ferguson, A. (1911). "Photographic measurements of Pendant Drops." Phil. Mag.Ser.6 **23**: 417-430.
[8] Ambwani, D. S., Fort Jnr, T. (1979). "Pendant: Drop Technique for Measuring Liquid Boundary Tensions." Surface and Colloid **11**: 93-119.
[9] Girault, H. H. J., Schiffrin, D.J., Smith, B.D.V. (1984). "The Measurement of Interfacial Tension of Pendant Drops using a Video Image Profile Digitizer." Journal of Colloid and Interfaces Sci **101, 1**: 257-266.
[10] Hauser, E., H. Edgerton, et al. (1936). "The Application of the High-speed Motion Picture Camera to Research on the Surface Tension of Liquids." The Journal of Physical Chemistry **40**(8): 973-988
[11] Hoorfar, M. and A. W. Neumann (2006). "Recent progress in axisymmetric drop shape analysis (ADSA)." Advances in colloid and interface science **121**(1-3): 25-49